동적 경화된 PP/EPDM 블렌드에서 PP 결정화 동역학의 *In-situ* 분석

Lei Hu, Bin Yang†, Yan-Li Deng, Fei-Xue Lu, Ru Xia, Zheng-Zhi Zheng, Ji-Bin Miao, Jia-Sheng Qian, Chuan-Ru Zhang*, Peng Chen, and Yu-Chuan Zhang

College of Chemistry & Chemical Engineering,
Anhui Provincial Key Laboratory of Environment-friendly Polymer Materials, Anhui University
*Department of Injection Molding, Longxing Automotive Components Co., Ltd.
(2016년 11월 15일 접수, 2017년 2월 11일 수정, 2017년 2월 14일 채택)

A Novel Kinetic Analysis of Crystallization of Polypropylene (PP) in Dynamically-vulcanized PP/Ethylene-propylene-diene Rubber (EPDM) Blends Using an *In-situ* Measurement Technique

Lei Hu, Bin Yang†, Yan-Li Deng, Fei-Xue Lu, Ru Xia, Zheng-Zhi Zheng, Ji-Bin Miao, Jia-Sheng Qian, Chuan-Ru Zhang*, Peng Chen, and Yu-Chuan Zhang

College of Chemistry & Chemical Engineering, Anhui Provincial Key Laboratory of Environment-friendly Polymer Materials, Anhui University, Hefei 230601, China
Department of Injection Molding, Longxing Automotive Components Co., Ltd., Lu'an, 237001, Anhui, China
(Received November 15, 2016; Revised February 11, 2017; Accepted February 14, 2017)

Abstract: The effects of cooling medium temperatures and plastic/rubber ratios on solidification and crystallization kinetics of dynamically-vulcanized polypropylene/ethylene-propylene-diene rubber (PP/EPDM) blends were investigated with the aid of an *in-situ* measurement technique. The cooling medium temperature heavily influenced the solidification kinetics primarily due to a combination of latent heat liberated from the molten polymer and the heat transferred away via the metallic wall during the cooling period. Interestingly, the parameter *C* in three-parameter model was not only affected by the material properties, but also by the cooling condition, different from the previous literature. The crystallization kinetics analysis indicated that the effect of EPDM in the blends consisted of both nucleation-promoting effect (low EPDM loading) and steric effect (higher EPDM loading). The present kinetic analysis may be helpful to further studies on improving the product performances for industrial applications.

Keywords: dynamic vulcanization, PP/EPDM blends, solidification kinetics, crystallization kinetics, cooling medium temperature.

Introduction

Polypropylene (PP), as a semi-crystalline thermoplastic plastic, has many advantages (e.g., high resistance to impact, good mechanical properties, resistance to a variety of organic solvents, etc), which has great applications in modern industry.[1-3] However, PP also has some drawbacks, such as high shrinkage ratio, high dielectric constant, and hence greatly limits its wide application.[4-6] Ethylene-propylene-diene rubber (EPDM) composed of ethylene, propylene and non-conjugated diene, which can improve physical properties, such as stiffness, heat distortion temperature and dimensional stability, etc.[7-10] Based on a degree of compatibility between EPDM and PP, EPDM was used as a toughening modifier to prepare the dynamic-vulcanized PP/EPDM blends, which have many excellent performances, for instance, high temperature resistance, impact resistance and recyclable.[11-13] Dynamic vulcanization is a commonly used method of fabricating PP/EPDM blends, in which the EPDM phase is partially or fully vulcanized.

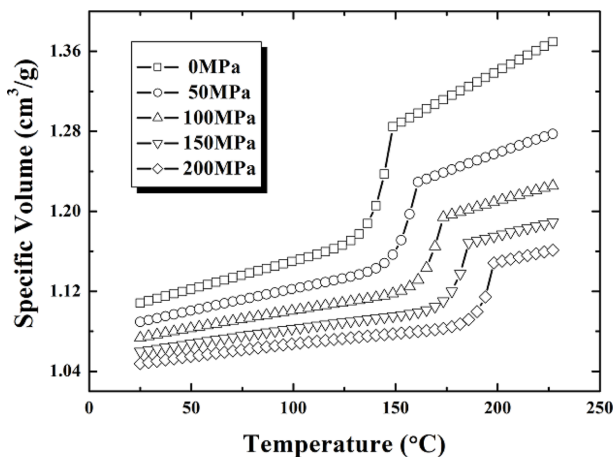The properties of semi-crystalline polymer were determined

Figure 1. The P-V-T curves of PP at equilibrium under various pressures.

by the mechanisms and kinetics involved, which had a close relationship with its crystallinity process.[14,15] The crystallization of polymer depended on many factors, such as, the molecular weight (M_w), the molecular weight distribution (MWD), and the cooling rate. Generally, due to the lack of *in-situ* instrument under the real operation conditions, to predict the cooling time during the melt cooling process was not easy. In our previous work, we developed a set of apparatus for real-time measurement during the cooling process for studying the phase-change behavior of polymer materials.[16-19] After several repeated tests, the apparatus showed good stability and reliability. Based upon those results, we here proposed a novel method to study the crystallization kinetics of PP in PP/EPDM blends and attempted to further explore the non-isothermal crystallization process of PP in the blends by using the solidification kinetic analysis coupled with the press-volume-temperature (P-V-T) relationship, as shown in Figure 1.

In this study, PP/EPDM blends with various EPDM contents were prepared by dynamic vulcanization technique. The effects of cooling medium temperature and EPDM content on the solidification and crystallization kinetics of PP in the blends were investigated extensively with an *in-situ* temperature measurement method. The study has practical significance for further exploring the crystallization kinetics and optimizing the process variables of crystalline polymers and their blends under real processing conditions.

Experimental

Materials. The polypropylene (PP, Grade: T30S) used in the present study was obtained from Petrochina Lanzhou Petrochemical Co., China with a melt flow index (MFI) of 2.84 g/10 min (under a loading of 2.16 kg at 230 °C), a solid density of 0.910 g/cm³ and a heat distortion temperature (HDT) of 114 °C. Ethylene-propylene-diene rubber (EPDM, Grade: 4785-HM) was supplied by Kairui Plastic Co., China. It contained 68% ethylene and 27% propylene. Dicumyl peroxide (DCP) was supplied by Hengnuo Chemical Technology (Yantai) Co., China.

Sample Preparation. Four weight ratios of PP/EPDM were employed in this study: 100/0, 90/10, 80/20 and 70/30. The blending successively began with PP, EPDM, DCP, and other boosters. DCP was added as a cross-linking agent in the samples. The samples were prepared in an internal mixer (a HAAKE torque rheometer) by melt mixing at a rotor speed of 60 rpm at 180 °C for 7 min. Then, the samples were moved from the internal mixer and mixed again for 15 min to prepare the blends on an open mill at 170 °C. Finally, the mixed blends were molded by dynamical vulcanizing technique on a press vulcanizer at 180 °C for 10 min and then cooled on another press vulcanizer at room temperature to prepare the specimens for subsequent characterization.

Experimental Procedures. The experimental set-up used in this work is illustrated in Figure 2. A certain amount of samples was put at the bottom of the metallic container. The bottom of the container was eventually heated to 220 °C and kept there for 10 min to ensure that the blends were uniformly melted. Subsequently, the metallic container was quickly immersed into a reservoir full of circulating water (as the cooling medium) whose temperature was controlled at a specific temperature (i.e., 20, 40, 60 and 80 °C, respectively). Meanwhile, a micro-thermocouple (model: TK-247, measuring range: 0~350 °C, Anthone Electronics Co., China) was fixed on the
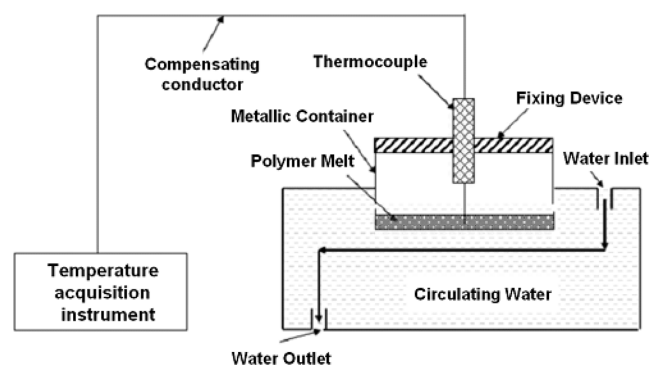

Figure 2. Schematic of experimental set-up for *in-situ* measurement of temperature.

top of the metallic container and inserted into the molten samples at a specific depth (close to the center of the molten materials). The decreases of melt temperature during the entire cooling stage were real-time recorded by a temperature acquisition instrument (model: LU-R2100, Anthone Electronics Co., China) through the compensating conductor with a sampling time of 1.0 s.

Results and Discussion

Solidification Kinetic Analysis of PP/EPDM Blends. As is known, a typical cooling process of the crystalline polymer undergoes three different stages:[17] liquid phase cooling stage, phase-change plateau and solid phase cooling stage, as shown in Figure 3. In stage I, the melt temperature decreased rapidly from the initial temperature (T_0) to the phase-change temperature (T_1-T_2) and the cooling rate decreased gradually. After that, in stage II, the melt temperature varied relatively slowly and the polymer melt began to change from liquid phase to
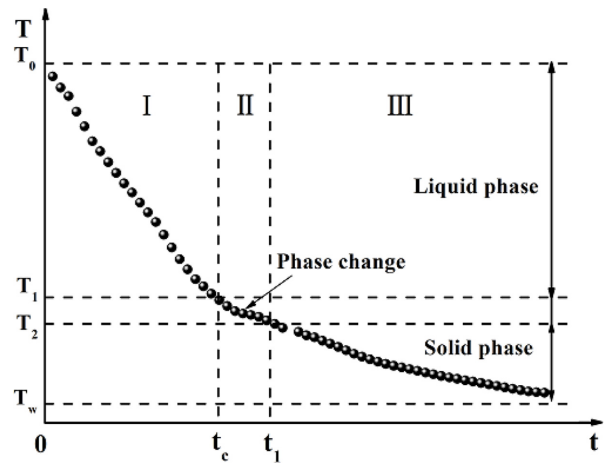
Figure 3. Schematic of a typical cooling curve for the crystalline polymer.

solid phase. Finally, in stage III, the cooling rate decreased as the cooling time elapsed and the curves tended to become flat. Thus, the melt temperature finally approached to the cooling
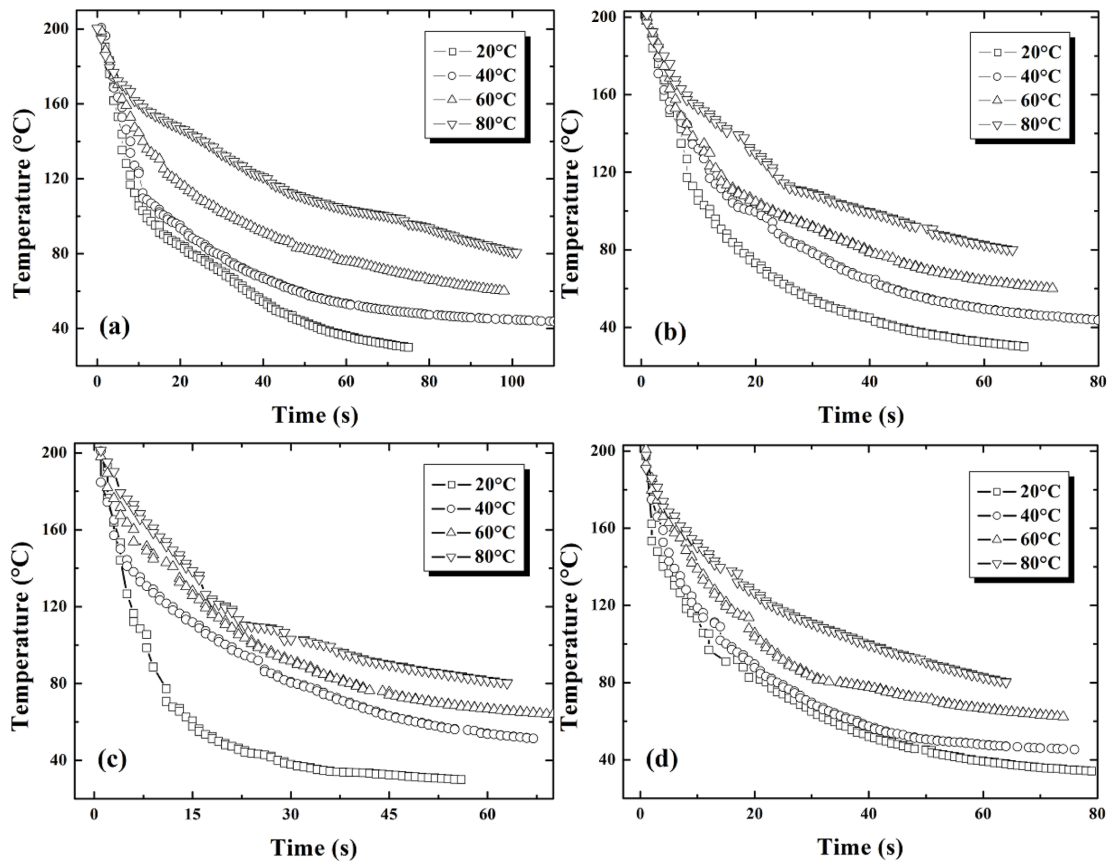
Figure 4. Temperature decay curves at different cooling medium temperature during cooling from melt state of (a) neat PP; (b) PP/EPDM (90/10); (c) PP/EPDM (80/20); (d) PP/EPDM (70/30).

medium temperature (T_w). The temperature profile would vary with cooling conditions, such as, the thermal properties of polymer, the temperature difference, etc.

The temperature decay curves of all samples cooled for various temperatures of the cooling medium during the whole cooling stage are presented in Figure 4. All cooling curves displayed similar shape. The melt temperature of the blends continued to fall until approaching the cooling medium temperature. The lower the temperature of the cooling medium, the faster the cooling rate was. The existence of the phase-change plateau was thus caused by the heat liberated from crystallization being equal to the heat transferred through the metallic container during the cooling process. Based on the previous work,[15-19] the crystallization rate was in proportion to the cooling rate. As the cooling rate increased, the crystallization took place much faster and hence the time of phase-change plateau lasted got much shorter.[19] Therefore, it can readily be seen that not all the curves displayed three stages. Because of the high thermal conductivity of metallic container

and the relatively greater temperature difference between the polymer melt and cooling medium, the latent heat released from the phase-change process can be easily transferred away to the cooling medium. Thus, no phase-change plateau can be observed in those curves. It can obviously be seen that the solidification and crystallization kinetics of PP/EPDM blends were strongly dependent on cooling medium temperature (T_w).

For better comprehension, a normalized temperature θ,[16] has been proposed in the solidification kinetic analysis, and can be defined as follows:

$$\theta = (T - T_w)/(T_0 - T_w) = \text{the dimensionless temperature} \quad (1)$$

where T, T_0 and T_w are the time dependent melt temperature, initial melt temperature, and cooling medium temperature, respectively.[16,17,20] Then, in order to further explore the physical factors behind the solidification kinetics of polymer, using a three-parameter model proposed in literature[17,18] through the non-linear fitting technique, the equation of the cooling curves
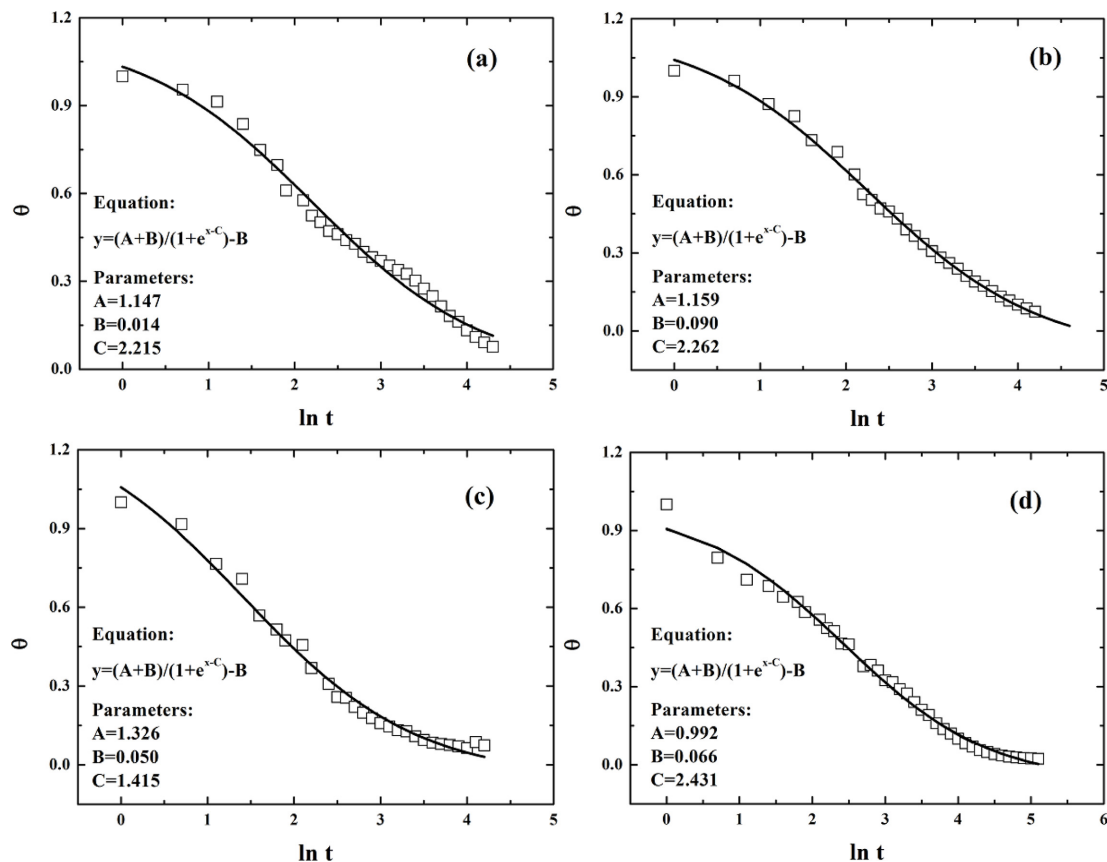

Figure 5. Non-linear curve fitting of experimental data using the three-parameter model at cooling medium temperature of 20 °C: (a) neat PP; (b) PP/EPDM (90/10); (c) PP/EPDM (80/20); (d) PP/EPDM(70/30).

can be summarized as:

$$\theta = (A + B)/(1 + e^{\ln t - C}) - B \qquad (2)$$

where parameter A is related to T_0, and B is determined by T_w. While parameter C is influenced by the molecular structure of the polymers, such as M_w, MWD, chain branching structure, etc. A smaller value of C always means shorter time for the melt to reach the cooling medium temperature.[16,17] The relationships of θ and $\ln t$ of the blends are presented in Figures 5-8. It was obvious that all curves had quite similar trends. Table 1 demonstrates the variations of the parameters A, B, C and values of the respective regression coefficient (R^2) with increasing EPDM content and cooling medium temperature. All values of R^2 were greater than 0.990, which indicated that the fitting accuracy of the curves were high for the non-linear curve fitting, as presented in Table 1. Moreover, it was obvious that A basically remained a constant value (~1.1) when the EPDM content and cooling medium temperatures varied in

this study. The value of B basically increased when cooling medium temperature rose for a given sample. For the blends at a given cooling medium temperature (e.g., 80 °C), the values of C ranked as: PP/EPDM (80/20) > PP/EPDM (70/30) > PP/EPDM (90/10) > neat PP. However, unlike previous literature, the parameter C in our study was found to be not just influenced by material characteristics of the polymers (e.g., molecular weight, thermal conductivity, etc.), but by the cooling conditions (e.g., cooling medium temperature). However, the reason why the varied value of C was associated with the EPDM content and cooling medium temperature still needed to be investigated. According to Table 1 and Figures 5-8, the experimental cooling curves of all samples agree quite well with their respective non-linear fitting curves.

From the practical view point, the value of cooling time (t_c), i.e., the time needed for cooling the polymer melt from T_0 to HDT, can be estimated for crystalline polymers during cooling process.[15] The t_c can readily be calculated using eq. (2), when the heat distortion temperature (HDT) of the polymer is given

Figure 6. Non-linear curve fitting of experimental data using the three-parameter model at cooling medium temperature of 40 °C: (a) neat PP; (b) PP/EPDM (90/10); (c) PP/EPDM (80/20); (d) PP/EPDM (70/30).
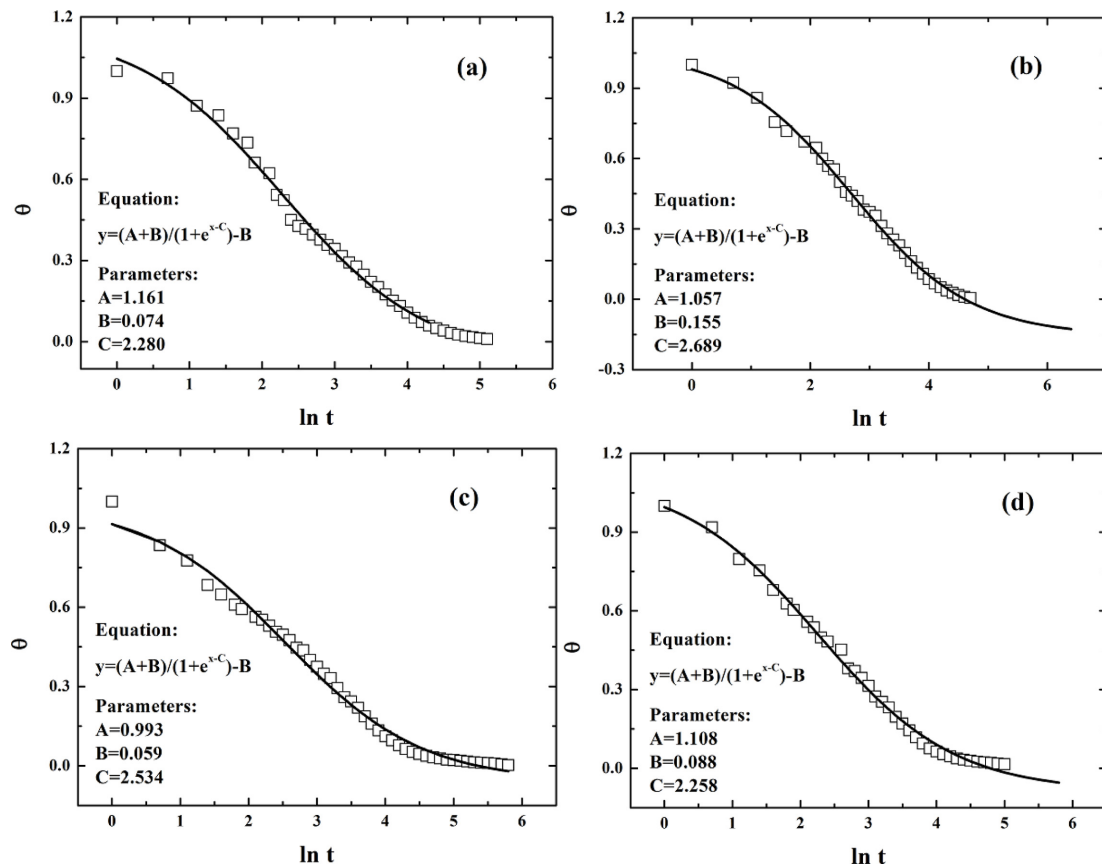
Figure 7. Non-linear curve fitting of experimental data using the three-parameter model at cooling medium temperature of 60 °C: (a) neat PP; (b) PP/EPDM (90/10); (c) PP/EPDM (80/20); (d) PP/EPDM(70/30).

Figure 8. Non-linear curve fitting of experimental data using the three-parameter model at cooling medium temperature of 80 °C: (a) neat PP; (b) PP/EPDM (90/10); (c) PP/EPDM (80/20); (d) PP/EPDM(70/30).
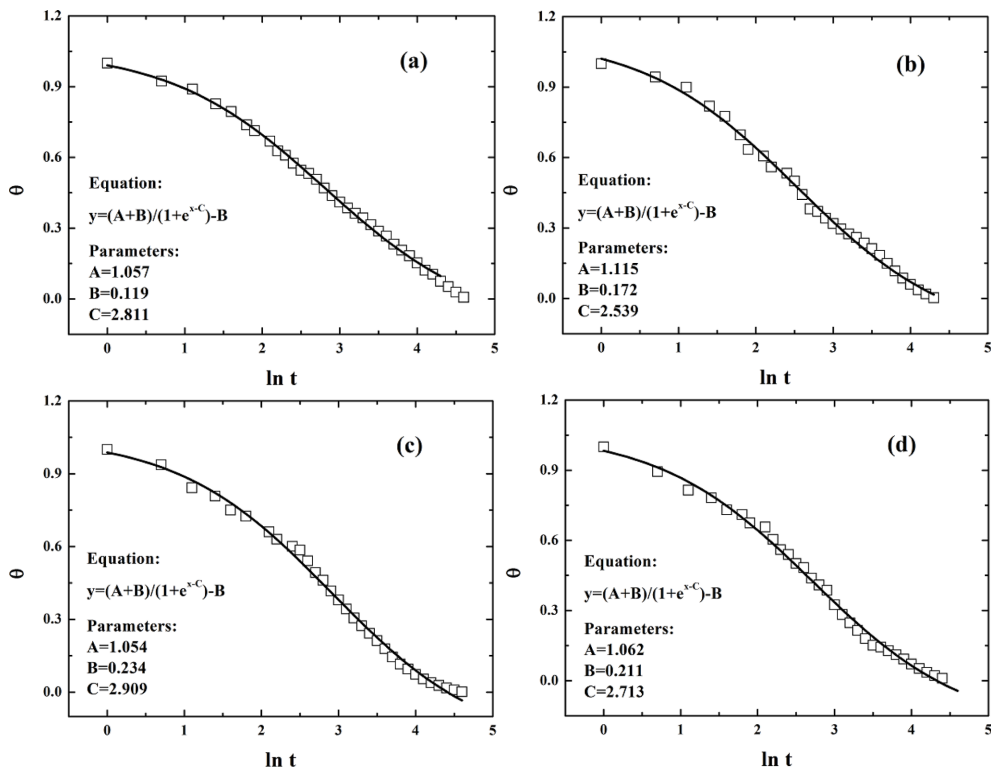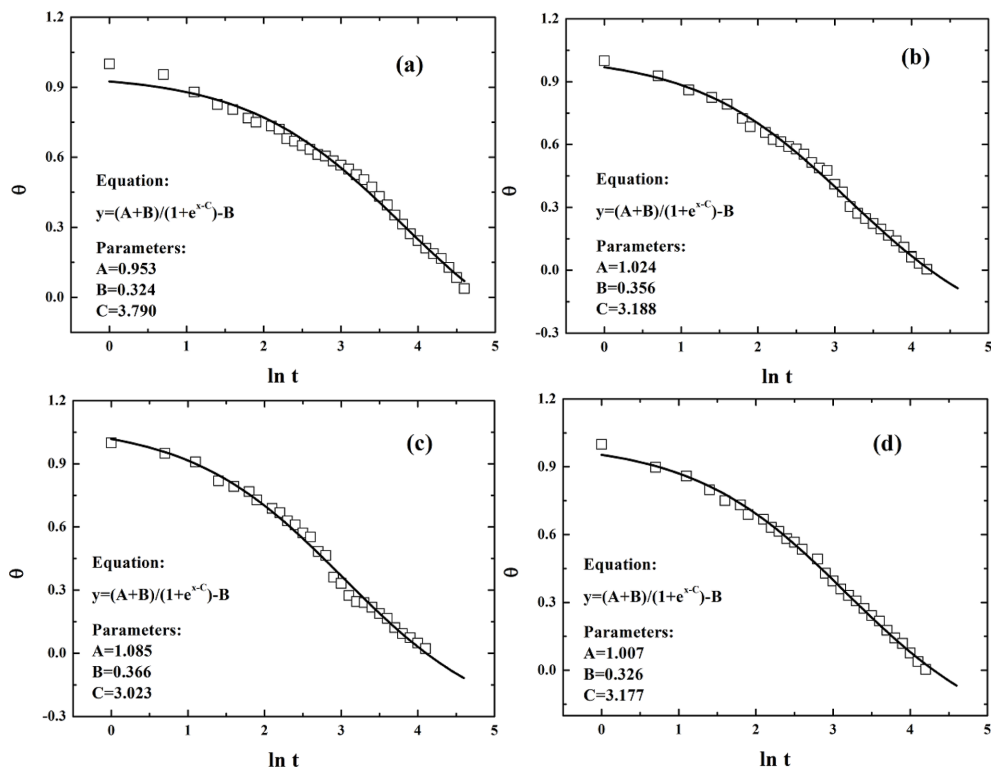
Table 1. Variation of the Parameters *A*, *B*, *C* and Regression Coefficient (R^2) with Different EPDM Contents and Cooling Medium Temperatures of PP/EPDM Blends

Temperature (°C)	Samples	*A*	*B*	*C*	R^2
20	PP	1.147	0.014	2.215	0.985
	PP/EPDM(90/10)	1.159	0.090	2.262	0.996
	PP/EPDM(80/20)	1.326	0.050	1.415	0.990
	PP/EPDM(70/30)	0.992	0.066	2.431	0.991
40	PP	1.159	0.077	2.290	0.993
	PP/EPDM(90/10)	1.057	0.155	2.689	0.997
	PP/EPDM(80/20)	0.993	0.059	2.534	0.990
	PP/EPDM(70/30)	1.108	0.088	2.258	0.996
60	PP	1.046	0.153	2.896	0.998
	PP/EPDM(90/10)	1.115	0.172	2.539	0.996
	PP/EPDM(80/20)	1.054	0.234	2.909	0.996
	PP/EPDM(70/30)	1.062	0.211	2.713	0.995
80	PP	0.953	0.324	3.790	0.989
	PP/EPDM(90/10)	1.024	0.356	3.188	0.996
	PP/EPDM(80/20)	1.085	0.366	3.023	0.993
	PP/EPDM(70/30)	1.007	0.326	3.177	0.997

Table 2. Comparison of Calculated and Experimental Cooling Times (t_c) of the Samples

Temperature (°C)	Samples	Cooling times (t_c) (s)	
		Calculated values	Experimental values
20	PP	11.47	8.7
	PP/EPDM(90/10)	10.9	8.8
	PP/EPDM(80/20)	6.3	6.0
	PP/EPDM(70/30)	10.1	10.0
40	PP	9.7	10.9
	PP/EPDM(90/10)	14.2	13.0
	PP/EPDM(80/20)	12.8	13.3
	PP/EPDM(70/30)	11.2	11.0
60	PP	22.2	21.9
	PP/EPDM(90/10)	16.6	14.7
	PP/EPDM(80/20)	19.8	19.1
	PP/EPDM(70/30)	17.1	17.7
80	PP	48.8	45.1
	PP/EPDM(90/10)	28.1	25.3
	PP/EPDM(80/20)	25.4	21.9
	PP/EPDM(70/30)	28.5	27.0

(measured). To be specific, the t_c can be jointly solved by $\theta_{HDT} = (HDT-T_w)/(T_0-T_w)$ coupled with $\theta_{HDT} = (A+B)/(1+e^{\ln t_c - C}) - B$, since the values of *A*, *B* and *C* should be earlier determined by non-linear curve fitting technique.

The ultimate temperature for usage of products was widely adopted as the demolding (or ejection) temperature during an industrial injection molding process. The experimental cooling time was in good agreement with the predicted t_c, as demonstrated in Table 2. The cooling time shortened with decreasing cooling medium temperature, which was mainly caused by the large temperature difference and great thermal conductivity. Thus, the cooling rate increased with decreasing cooling medium temperature. The t_c can be simply predicted by the three-parameter model, which can supply good insight into the formation of various crystalline structures as well as the optimization of processing variable of cooling process.

Crystallization Kinetics of PP Phase in PP/EPDM Blends. The developments of relative crystallization with the crystallization time of the samples were presented in Figure 9. To explore the physical reason behind the crystallization process of PP/EPDM blends, the density equation was utilized in the present work.[18,21] The relative crystallinity (X_t) at time t during the crystallization process can be calculated[18] as below:

$$X_t = \rho_c/\rho \cdot (\rho-\rho_a)/(\rho_c-\rho_a) \times 100\% = (V_a-V)/(V_a-V_c) \times 100\% \quad (3)$$

where ρ_c, ρ_a, V_c and V_a are the four parameters associated with polymer crystallization process.[17,21,22] ρ_c and ρ_a are the densities of fully crystalline and amorphous regions of PP, respectively. Similarly, V_c and V_a denote the specific volume of fully crystalline and amorphous phases, respectively. These all curves were in the shape of "S" in Figure 9, which indicated a fast primary process during the initial stage and a slow secondary process during the later stage.[15] The relative crystallinity got a jump after an induction period, which was continued by a stage when the relative crystallinity increased slowly and gradually reached a maximum at the end of the total crystallization period.[23]

As can be seen in Figure 9, the crystallization rates of the blends became significantly higher with decreasing the cooling medium temperature, which were mainly concerned with the cooling rate during cooling process. One important parameter about crystallization kinetic is the crystallization half-time ($t_{1/2}$), which can be readily obtained from the relative degree of crystallinity plotted as a function of time (cf. Figure 9). $t_{1/2}$ is the change of time from the initial time to the time when the X_t
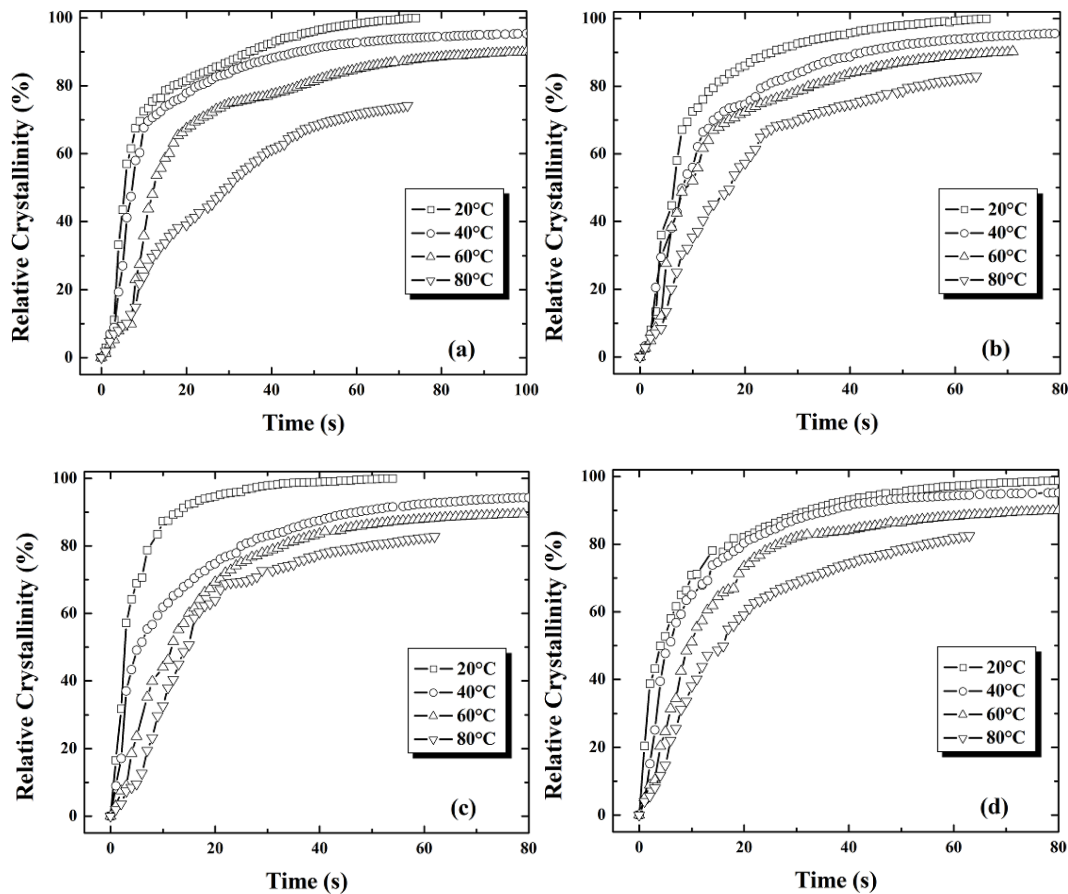
Figure 9. The melt crystallization kinetic curves at different cooling medium temperatures during non-isothermal cooling period: (a) neat PP; (b) PP/EPDM (90/10); (c) PP/EPDM (80/20); (d) PP/EPDM (70/30).

Table 3. Effect of EPDM Content on Crystallization Half-time ($t_{1/2}$) of PP in the Blends

Temperature (°C)	Values of $t_{1/2}$ (s)			
	PP	PP/EPDM (90/10)	PP/EPDM (80/20)	PP/EPDM (70/30)
20	5.49	6.39	2.71	4.01
40	7.25	8.03	5.37	5.65
60	12.35	8.77	11.72	9.62
80	29.11	17.10	14.66	16.08

reaches 50%, which is usually utilized to characterize the crystallization rate.[23] Larger value of $t_{1/2}$ always indicates a lower crystallization rate (i.e., slower crystallization kinetics). All $t_{1/2}$ values of the blends are listed in Table 3. It was obvious that the values of $t_{1/2}$ of PP/EPDM blends at same cooling medium temperature were basically less than those of neat PP during the non-isothermal crystallization process, indicating that EPDM played a good role in promoting the crystallization of PP phase.[22,24] It seemed that there were likely more nucleating

sites in the blends when EPDM particles were dispersed in the PP matrix. The incorporation of EPDM improved the crystallization rate at low content, but the promoting effect was related to the content of EPDM in the blends.[25] With the EPDM content continually increasing, the crystallization of PP phase was restricted by the dispersed EPDM particles, leading to the reduced crystallization rate and low degree of crystallinity.[26-29] For instance, at same medium temperature, the $t_{1/2}$ of the blend (20% EPDM) was found to be smallest, which showed a high non-isothermal crystallization rate and the most active nucleation promotion effect of PP phase among these blends. It was mainly caused by the limited space for the further growth of crystal in the blends. EPDM with the large number of branching chains might act as a blocking agent, increase the viscosity of the blends and decrease the chain motion. Hence, the motion of PP chains toward the growing nuclei became more difficult. Moreover, interactions such as hydrogen bonding between polar groups of branching chains became stronger with increasing EPDM content, and would

cause more physically crosslinking network to form in the blends. Consequently, the crystallization rate decreased remarkably at higher EPDM content in the blends. Thus, it can be concluded that the effects of EPDM particles on the crystallization of PP phase in the blends mainly consisted of the promoting nucleation effect (related to crystal nucleation) and steric effect (primarily influencing the crystal growth).

In addition, interestingly, when cooling medium temperature was 60 °C, the $t_{1/2}$ of PP/EPDM (80/20) blends was large, which will be further investigated in our ongoing work. The obtained data (cf. Table 3) also showed that the values of $t_{1/2}$ of same blend increased as cooling medium temperature increased, indicating that the crystallization kinetics of the blends were strongly affected by the cooling medium temperature. The crystallization rate decreased with increasing cooling medium temperature, which was consistent with earlier discussions.

Conclusions

In the article, a novel method was applied to study the solidification and crystallization kinetics of PP/EPDM blends. Investigation on the effects of cooling medium temperatures and plastic/rubber ratios on the solidification kinetic as well as crystallization kinetics of the PP/EPDM blends were performed using an *in-situ* measurement of the temperature decay. It revealed that the cooling medium temperature strongly influenced the solidification kinetics of the blends, which could be attributed to the combination between heat liberated from crystallization and the heat transferred through the metallic container during cooling process. Our experimental results were in good agreement with the theoretical predictions using three-parameter model. Interestingly, the parameter C was not merely influenced by the materials properties, but also by the cooling conditions, which differed from the previous findings. The crystallization kinetics study presented that the incorporation of EPDM to PP matrix promoted the nucleation process of PP, leading to the increased crystallization rate. Especially, the value of $t_{1/2}$ of the PP/EPDM (80/20) blend was basically smallest at same cooling medium temperature, indicating the fastest crystallization rate among the blends. However, the crystallization rate of the blend with a higher EPDM content decreased slightly. In conclusion, the EPDM effects on the crystallization kinetics of PP phase in the blends mainly depended on the promoting nucleation effect and steric effect. The present study has significance for further exploring the crystallization kinetics and optimizing process parameters of the blends during real processing operations.

References

1. N. G. Karsli, S. Yesil, and A. Aytac, *Compos. Part B: Eng.*, **63**, 154 (2014).
2. J. Lee, H. Kim, and H. J. Kang, *Polym. Korea*, **36**, 803 (2012).
3. M. Lazaar, S. Bouadila, S. Kooli, and A. Farhat, *Appl. Therm. Eng.*, **68**, 62 (2014).
4. L. Mariem, B. Salwa, K. Sami, and F. Abdelhamid, *Appl. Therm. Eng.*, **68**, 62 (2014).
5. G. Kim, I. K. Park, S. H. Kim, Y. Kim, H. W. Seo, J. H. Yun, S. H. Kim, D. K. Kim, and J. D. Nam, *Polym. Korea*, **40**, 313 (2016).
6. L. Gong, B. Yin, L. P. Li, and M. B. Yang, *J. Macromol. Sci. Phys.*, **50**, 806 (2011).
7. B. S. Shin, S. T. Jung, J. P. Jeun, H. B. Kim, S. H. Oh, and P. H. Kang, *Polym. Korea*, **36**, 549 (2012).
8. M. Tian, X. L. Zhang, L. Q. Zhang, S. Yin, T. Nishi, and N. Y. Ning, *Compos. Sci. Technol.*, **79**, 21 (2013).
9. Q. S. Zhen, C. Li, L. Ling, C. L. Deng, J. Zhao, and Y. Z. Wang, *Ind. Eng. Chem. Res.*, **52**, 8454 (2013).
10. A. Thompson, O. Bianchi, C. L. G. Amorim, C. Lemos, S. R. Teixeira, D. Samios, C. Giacomelli, J. S. Crespo, and G. Machado, *Polymer*, **52**, 1037 (2011).
11. L. Gong, B. Yin, L. P. Li, and M. B. Yang, *J. Appl. Polym. Sci.*, **123**, 510 (2012).
12. L. F. Ma, W. K. Wang, and R. Y. Bao, *Mater. Design*, **51**, 536 (2013).
13. D. M. Stelescu, A. Airinei, M. Homocianu, N. Fifere, D. Timpu, and M. Aflori, *Polym. Test.*, **32**, 187 (2013).
14. K. H. Yoon, D. Y. Shin, and Y. C. Kim, *Polym. Korea*, **36**, 245 (2012).
15. B. Yang, J. Z. Lin, R. Xia, L. F. Su, J. B. Miao, J. S. Qian, P. Chen, J. W. Liu, and S. Q. Deng, *J. Macromol. Sci.; Part B: Polym. Phys.*, **53**, 462 (2014).
16. B. Yang, G. J. Li, M. B. Yang, L. F. Su, J. B. Miao, R. Xia, P. Chen, S. Q. Deng, and J. S. Qian, *J. Res. Updates Polym. Sci.*, **2**, 1 (2013).

17. B. Yang, X. R. Fu, W. Yang, N. Sun, S. Hu, L. Ying, and M. B. Yang, *J. Macromol. Sci.; Part B: Polym. Phys.*, **49**, 734 (2010).

18. B. Yang, R. Xia, J. B. Miao, J. S. Qian, M. B. Yang, and P. Chen, *Polym. Test.*, **32**, 202 (2013).

19. B. Yang, J. B. Miao, K. Min, R. Xia, J. S. Qian, and X. Wang, *J. Appl. Polym. Sci.*, **128**, 1922 (2013).

20. S. P. Tao, X. R. Fu, M. B. Yang, and R. Z. Yu, *Acta Polym. Sin.*, **1**, 8 (2005).

21. M. Sattari, A. Molazemhosseini, and M. R. Naimi-Jamal, *Mater. Chem. Phys.*, **147**, 942 (2014).

22. L. Hu, B. Yang, R. Xia, J. B. Miao, F. X. Lu, M. Cao, J. S. Qian, and Y. C. Zhang, *Adv. Mater. Res.*, **1078**, 8 (2015).

23. C. W. Wang and C. Q. Li, *China Synthetic Rubber Ind.*, **35**, 124 (2012).

24. L. Huang, L. Hu, B. Yang, J. B. Miao, R. Xia, J. S. Qian, and M. Cao, *Mater. Sci.*, **4**, 205 (2014).

25. Y. Zare and H. Garmabi, *J. Appl. Polym. Sci.*, **124**, 1225 (2012).

26. C. M. Huang, H. W. Bai, H. Xiu, Q. Zhang, and Q. Fu, *Compos. Sci. Technol.*, **102**, 20 (2014).

27. H. W. Bai, D. Y. Bai, H. Xiu, H. L. Liu, Q. Zhang, K. Wang, H. Deng, F. Chen, Q. Fu, and F. C. Chiu, *RSC Adv.*, **4**, 49374 (2014).

28. F. Luo, K. Wang, N. Y. Ning, C. Z. Geng, H. Deng, F. Chen, Q. Fu, Y. Y. Qian, and D. Zheng, *Polym. Adv. Technol.*, **22**, 2044 (2011).

29. Y. L. Loo, R. A. Register, D. H. Adamson, and A. J. Ryan, *Macromolecules*, **38**, 4947 (2005).